

Inverted Grating Relief Atomic Clock VCSELs

Ahmed Al-Samaneh

Vertical-cavity surface-emitting lasers (VCSELs) with single-mode and single-polarization emission at a wavelength of 894.6 nm have become attractive light sources for miniaturized Cs-based atomic clocks. So far, VCSELs used for these applications are single-mode because of small active diameters which has the drawbacks of increased ohmic resistance and reduced lifetime. Employing surface grating reliefs, enhanced fundamental-mode emission as well as polarization-stable laser oscillation are achieved. VCSELs with 5 μm active diameter show side-mode suppression ratios of 20 dB even at currents close to thermal roll-over with orthogonal polarization suppression ratios better than 20 dB at elevated ambient temperatures up to 100°C.

1. Introduction

Over the last few years, microscale atomic clocks have emerged as a new application field of VCSELs. Owing to their enhanced accuracy and low power consumption compared to thermally stabilized quartz-based oscillators, such clocks are key elements in a wide range of systems and applications such as global positioning, synchronization of communication networks, or undersea exploration. The first demonstrations of microscale atomic clocks based on coherent population trapping (CPT) spectroscopy [1] and microelectromechanical system (MEMS) fabrication techniques were done separately at the National Institute of Standards and Technology (NIST) [2] and at Symmetricom [3], both in the USA in the year 2004. Such frequency sources have recently become commercially available [4]. VCSELs used in those clocks must feature single-mode, single-polarization, low noise, and narrow linewidth emission under harmonic modulation at about 4.6 GHz with a center wavelength of about 894.6 nm to employ the CPT effect of the cesium D1 line. VCSELs of this kind have already been developed [5–8]. Our own research [6–8] has targeted the use in the first European microscale atomic clock demonstrators [9]. The polarization and dynamic properties of the lasers are reported in [7]. For polarization control, a semi-conducting surface grating is etched in the top Bragg mirror. In particular, so-called inverted grating VCSELs have been employed where the grating is etched in an extra topmost GaAs quarter-wave antiphase layer [10]. These VCSELs are single-mode because of a small active diameter, e.g., 3 to 4 μm , which is achieved by wet-chemical oxidation of a thin AlAs layer grown above the active region. However, VCSELs with small active diameters have the drawbacks of increased ohmic resistances and reduced lifetimes owing to higher current densities and possibly increased internal temperatures resulting from higher thermal and electrical resistances. Oxide-confined VCSELs with larger active diameter showing single transverse mode oscillation can be realized by, e.g., etching a

shallow surface relief in the top Bragg mirror of a regular VCSEL structure [11] (alternative approaches are summarized in [12]). An annular etch of the laser outcoupling facet lowers the effective mirror reflectivity particularly for higher-order modes, which show higher optical intensities outside the device center. The resulting differences in threshold gains strongly favor the fundamental mode. A more advanced approach is to etch the surface relief in an extra topmost GaAs quarter-wave antiphase layer, leading to the so-called inverted relief VCSELs. Here, the antiphase layer is removed only in the center of the outcoupling facet, and consequently the threshold gain for the fundamental mode is most strongly decreased. This approach requires a less precise etch depth control and has been successfully demonstrated in [13] with maximum single-mode output powers of up to 6.3 mW. So-called inverted grating relief VCSELs combine a surface grating and a surface relief in an extra topmost antiphase layer. Such a combination results simultaneously in a favorable single-mode and polarization-stable laser emission [14]. In this article, the design, fabrication, characterization, and preliminary reliability test results of inverted grating relief VCSELs are presented.

2. VCSEL Design and Fabrication

The VCSELs are grown by solid-source molecular beam epitaxy on n-doped (100)-oriented GaAs substrates. The layer structure of the VCSELs is similar to the one described in [7]. There is a highly n-doped GaAs contact layer above the GaAs substrate to allow n-contacting. The active region contains three compressively strained InGaAs quantum wells with 4% indium content and is positioned in an optical cavity between doped distributed Bragg reflectors (DBRs). The n- and p-type DBRs consist of 38.5 Si-doped $\text{Al}_{0.2}\text{Ga}_{0.8}\text{As}/\text{Al}_{0.9}\text{Ga}_{0.1}\text{As}$ layer pairs and 25 C-doped layer pairs with identical composition, respectively. The DBRs are graded in composition and doping concentration to minimize the free-carrier absorption and decrease the electrical resistance. A 30 nm thick AlAs layer is grown above the active region. It is wet-chemically oxidized to achieve current confinement and optical index guiding. To maximize compactness in the clock microsystem, flip-chip-bondable VCSEL chips have been realized, similar to the ones described in [6, 7]. The structure has an extra topmost quarter-wave thick GaAs layer to achieve an antiphase reflection for all modes. By etching a circular area of 3 to 4 μm diameter in the center of this layer, the reflectivity is increased particularly for the fundamental mode. If instead a grating with the same extension is etched into the topmost layer (see Fig. 1), this additionally leads to different reflectivities for the two polarizations of the fundamental mode. Inverted grating reliefs with quarter-wave etch depth, sub-emission-wavelength grating periods (specifically 0.6 μm), and 50% duty cycle have been employed. The grating grooves are etched along the [011] crystal axis.

3. Operation Characteristics and Spectra

The VCSELs to be incorporated in miniaturized atomic clock microsystems will experience high ambient temperatures (e.g., $T = 65 \dots 80^\circ\text{C}$). The polarization-resolved light-current-voltage (PR-LIV) characteristics of a grating relief VCSEL with 4.5 μm active

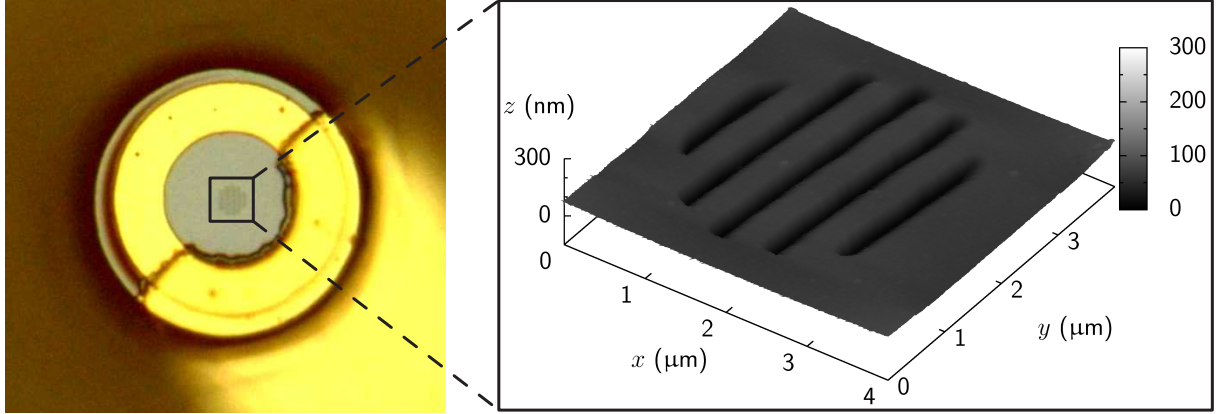


Fig. 1: Optical micrograph of a fully processed VCSEL with an inverted grating relief (left) and its surface profile measured with an atomic force microscope (right). The grating relief has a diameter of 3 μm, a grating period of 0.6 μm, and an etch depth of 70 nm.

diameter at 80 °C substrate temperature are shown in Fig. 2 (left). The dashed and dash-dotted lines indicate the optical powers P_{orth} and P_{par} measured behind a Glan–Thompson polarizer whose transmission direction is oriented orthogonal and parallel to the grating lines, respectively. The device remains polarization-stable up to thermal roll-over with a maximum magnitude of the orthogonal polarization suppression ratio (OPSR) as high as 19.5 dB, where $\text{OPSR} = 10 \log(P_{\text{par}}/P_{\text{orth}})$. Figure 2 (right) depicts polarization-resolved spectra at 80 °C. The target wavelength is reached at a current of 3.8 mA with both a side-mode suppression ratio (SMSR) and a peak-to-peak difference between the dominant and the suppressed polarization modes of almost 27 dB, which well exceed the target values of 20 dB.

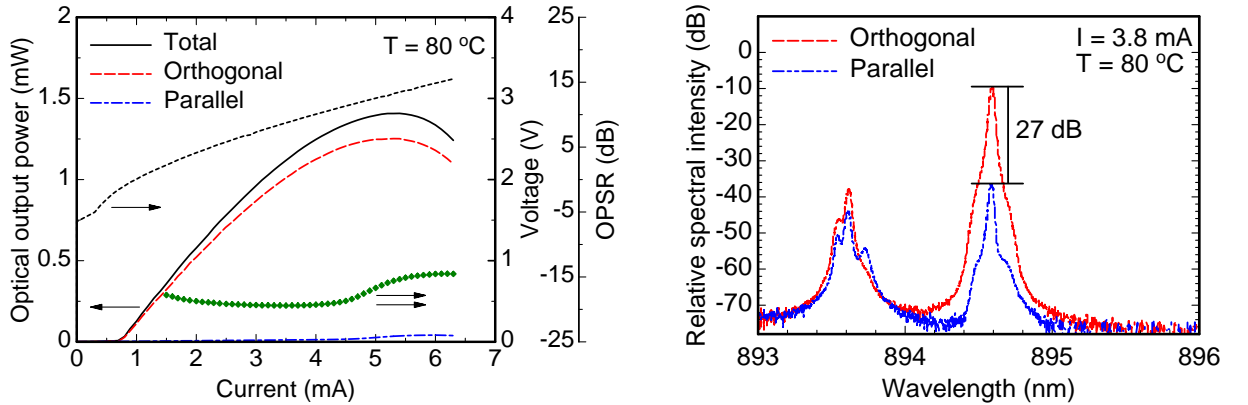


Fig. 2: Polarization-resolved operation characteristics of a grating relief VCSEL with 4.5 μm active diameter at 80 °C substrate temperature (left). Polarization-resolved spectra of the same VCSEL at 3.8 mA bias current (right). The grating relief has a diameter of 3.3 μm.

The polarization control induced by the grating relief has also been investigated for different ambient temperatures. Figure 3 depicts PR-LIV characteristics of a grating relief VCSEL with 5 μm active diameter for substrate temperatures varied between 20 and

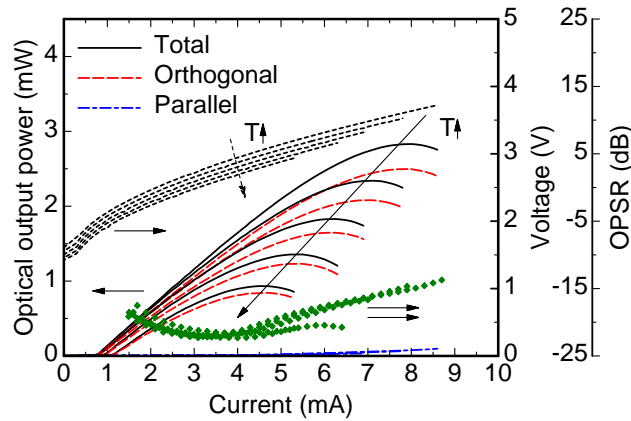


Fig. 3: Polarization-resolved operation characteristics of a grating relief VCSEL with $5\ \mu\text{m}$ active diameter at substrate temperatures from 20 to $100\ ^\circ\text{C}$ in steps of $20\ ^\circ\text{C}$. The grating relief has a diameter of $4\ \mu\text{m}$.

$100\ ^\circ\text{C}$ in steps of $20\ ^\circ\text{C}$. As can be seen, the VCSEL remains polarization-stable even well above thermal roll-over. The magnitudes of the OP SR for $T = 80$ and $100\ ^\circ\text{C}$ are increased in comparison with lower temperatures as the current exceeds $4.5\ \text{mA}$.

For investigating the enhancement of fundamental-mode emission, standard reference devices were fabricated on the same wafer adjacent to the grating relief VCSELs for comparison purposes. For the reference VCSELs, the topmost GaAs quarter-wave antiphase layer is etched over the whole outcoupling facet. This means that in-phase reflection is achieved for all modes. The reference VCSELs can thus be considered as standard VCSELs. Figure 4 displays the PR-LI characteristics of a reference device with an oxide

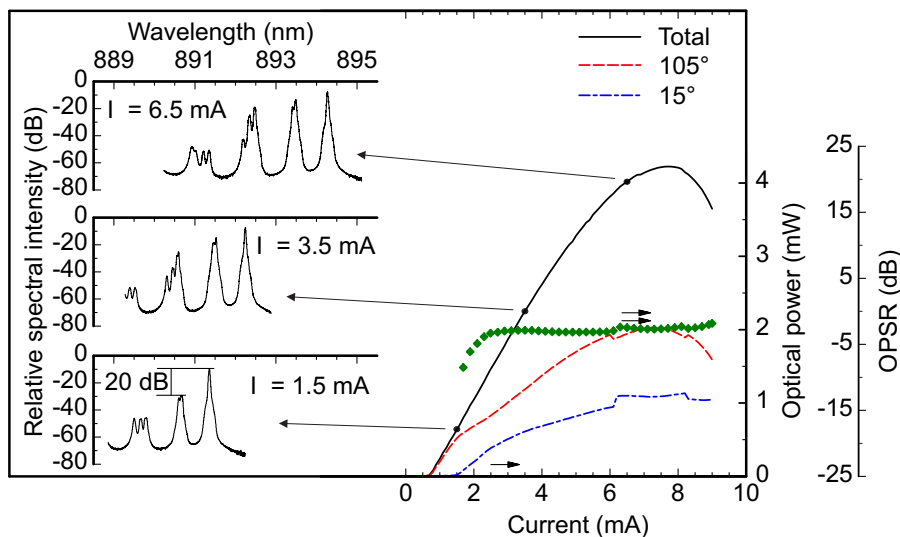


Fig. 4: Polarization-resolved operation characteristics of a reference VCSEL with $5\ \mu\text{m}$ active diameter at $80\ ^\circ\text{C}$ substrate temperature. The emission spectra in the insets show higher-order lasing modes. The polarization directions of the two orthogonal, linearly polarized fundamental modes are rotated by 15° towards the $[0\bar{1}1]$ axis.

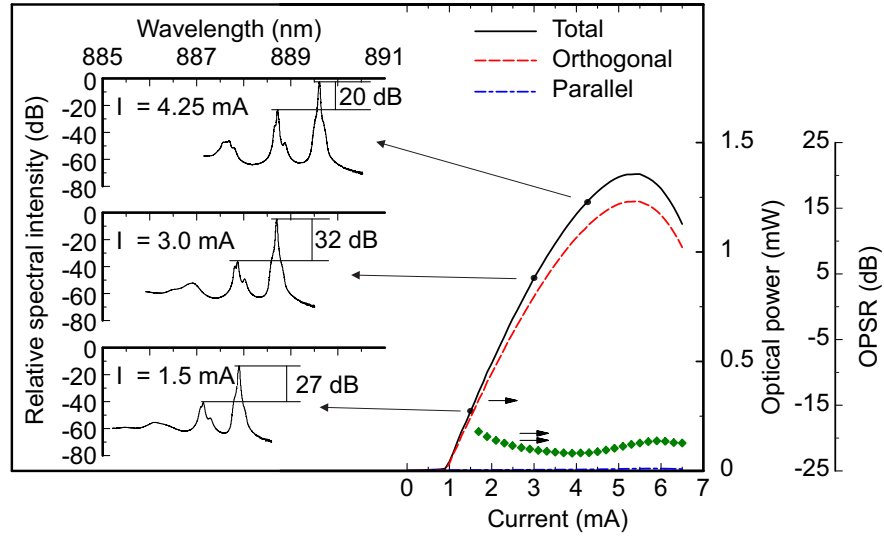


Fig. 5: Polarization-resolved operation characteristics of the grating relief VCSEL from Fig. 3 at 80 °C substrate temperature. The emission spectra in the insets show SMSRs of at least 20 dB.

aperture of about 5 μm at 80 °C substrate temperature and its optical spectra at different driving currents. The laser has a threshold current of 0.7 mA and a maximum output power of 4.2 mW. At 1.5 mA drive current it shows single-mode operation with an SMSR of 20 dB. However, the spectrum gets highly multimode for higher currents. Having no surface grating, the reference VCSEL shows a weak polarization control with an average OPSR of -4.1 dB. The OPSR is calculated for data points in steps of 0.1 mA and then averaged over the current range yielding 10% to 100% of the maximum output power. Due to built-in strain forces, the two orthogonal, linearly polarized fundamental modes are not aligned parallel and orthogonal to the usually preferred $[011]$ crystal axis. Instead, they are rotated by 15° towards the $[0\bar{1}1]$ axis because of the elasto-optic effect [15]. Figure 5 depicts the same measurements for a nearby laser (same as Fig. 3) on the same sample, which is nominally identical except for a surface grating relief with a diameter of 4 μm . The grating relief device shows an increased threshold current of 0.9 mA due to the effectively decreased mirror reflectivity. The optical spectra confirm SMSRs exceeding 20 dB up to 4.25 mA at which the laser delivers a maximum single-mode output power of 1.2 mW. This current is just 1.25 mA below the thermal roll-over point. Owing to the grating, the VCSEL is polarization-stable well above thermal roll-over with an average OPSR of -21 dB.

4. Reliability Test

For preliminary reliability testing, a sample containing several grating relief VCSELs was introduced in a setup in which six individual lasers with 5.5 (2 devices), 5.0, 4.4, 3.8 and 3.7 μm active diameter are operated at a constant current of 3 mA and 80 °C ambient temperature. The optical output power of each device is measured separately (while the other devices are switched off) using a 1 mm² area Si photodiode. The optical power was recorded every half hour for about 2500 hours. Figure 6 shows the output power versus

time for all devices. Obviously such a small number of devices is not sufficient to obtain reliable lifetime estimations. Nevertheless, this preliminary test shows that all lasers kept to be functional with slower degradation of the devices with active diameters $\geq 5 \mu\text{m}$.

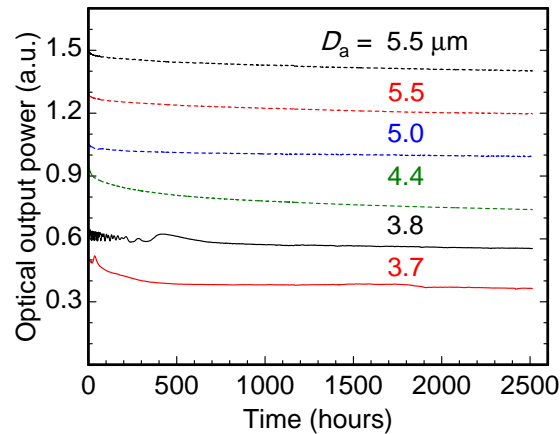


Fig. 6: Output power evolution in a long-term test of grating relief VCSELs with different active diameter D_a at 80°C and 3 mA constant current.

Figure 7 depicts the LIV characteristics of two VCSELs from Fig. 6 with $3.8 \mu\text{m}$ and $5 \mu\text{m}$ active diameter. Both lasers were measured at 80°C after 0, 100, 200, 500 and 2500 hours. The VCSEL with $3.8 \mu\text{m}$ active diameter suffers from an increase in threshold current from 0.6 to 0.87 mA (i.e., by 45%) with almost no change in the slope efficiency of about 0.48 W/A after 2500 hours of lifetime test. On the other hand, for the second VCSEL with $5 \mu\text{m}$ active diameter, the threshold current increases only from 0.84 to 0.91 mA (i.e., by 4.5%). Its slope efficiency decreases from 0.43 to 0.39 W/A after the same test time, where the change occurs mainly during the first 100 hours of operation. It can thus be expected that lasers with $5 \mu\text{m}$ active diameter provide greater potential for increased lifetime in comparison with standard small-aperture single-mode devices with 3 to $4 \mu\text{m}$

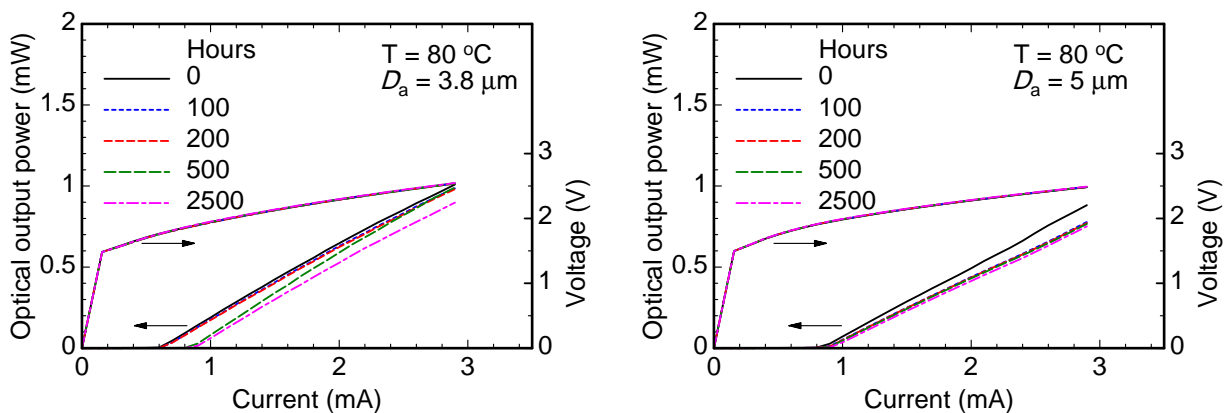


Fig. 7: Operation characteristics of the VCSEL with $3.8 \mu\text{m}$ active diameter (left) and of the VCSEL with $5 \mu\text{m}$ diameter from Fig. 6 measured at 80°C during the reliability test at 0, 100, 200, 500 and 2500 hours.

active diameters. For both lasers the voltage characteristics remain almost unchanged during the degradation test time.

5. Conclusion

In summary, inverted grating relief VCSELs emitting at 894.6 nm wavelength have been fabricated for Cs-based miniature atomic clocks. Their emission is stable on the fundamental mode with a fixed linear polarization. VCSELs with 5 μm active diameter show side-mode suppression ratios of 20 dB even at currents close to thermal roll-over with orthogonal polarization suppression ratios better than 20 dB at elevated ambient temperatures up to 100 °C. Preliminary lifetime tests confirm a better reliability of these VCSELs compared to those which are single-mode due to small oxide apertures.

Acknowledgments

The author would like to cordially thank Y. Men for performing the electron-beam lithography step for grating fabrication. He wishes to thank W. Schwarz and A. Hein for their technical assistance with lifetime measurements. This work is funded by the EC within FP7 (grant agreement number 224132, www.mac-tfc.eu).

References

- [1] N. Cyr, M. Têtu, and M. Breton, “All-optical microwave frequency standard: a proposal”, *IEEE Transactions on Instrumentation and Measurement*, vol. 42, no. 2, pp. 640–649, 1993.
- [2] S. Knappe, V. Shah, P. Schwindt, L. Hollberg, J. Kitching, L.A. Liew, and J. Moreland, “A microfabricated atomic clock”, *Appl. Phys. Lett.*, vol. 85, no. 9, pp. 1460–1462, 2004.
- [3] R. Lutwak, J. Deng, W. Riley, M. Varghese, J. Leblanc, G. Tepolt, M. Mescher, D.K. Serkland, K.M. Geib, and G.M. Peake, “The chip-scale atomic clock – low-power physics package”, in *Proc. 36th Annual Precise Time and Time Interval (PTTI) Meeting*, pp. 339–354. Washington, DC, USA, Dec. 2004.
- [4] W.D. Jones, “Chip-scale atomic clock”, *IEEE Spectrum*, Mar. 2011. Web page: <http://spectrum.ieee.org/semiconductors/devices/chipscale-atomic-clock>, last visited Apr. 2012.
- [5] D.K. Serkland, K.M. Geib, G.M. Peake, R. Lutwak, A. Rashed, M. Varghese, G. Tepolt, and M. Prouty, “VCSELs for atomic sensors”, in *Proc. SPIE*, vol. 6484, pp. 648406-1–10, 2007.

- [6] A. Al-Samaneh, S. Renz, A. Strodl, W. Schwarz, D. Wahl, and R. Michalzik, “Polarization-stable single-mode VCSELs for Cs-based MEMS atomic clock applications”, in *Semiconductor Lasers and Laser Dynamics IV*, Proc. SPIE 7720, pp. 772006-1–14, 2010.
- [7] A. Al-Samaneh, M. Bou Sanayeh, S. Renz, D. Wahl, and R. Michalzik, “Polarization control and dynamic properties of VCSELs for MEMS atomic clock applications”, *IEEE Photon. Technol. Lett.*, vol. 23, no. 15, pp. 1049–1051, 2011.
- [8] A. Al-Samaneh, M.T. Haidar, D. Wahl, and R. Michalzik, “Polarization-stable single-mode VCSELs for Cs-based miniature atomic clocks”, in *Online Digest Conf. on Lasers and Electro-Optics Europe, CLEO/Europe 2011*, paper CB.P.23, one page. Munich, Germany, May 2011.
- [9] C. Gorecki, M. Hasegawa, N. Passilly, R.K. Chutani, P. Dziuban, S. Gailliou, and V. Giordano, “Towards the realization of the first European MEMS atomic clock”, in Proc. *2009 IEEE/LEOS International Conference on Optical MEMS and Nanophotonics*, pp. 47–48. Clearwater, FL, USA, Aug. 2009.
- [10] J.M. Ostermann, P. Debernardi, and R. Michalzik, “Optimized integrated surface grating design for polarization-stable VCSELs”, *IEEE J. Quantum Electron.*, vol. 42, no. 7, pp. 690–698, 2006.
- [11] H.J. Unold, S.W.Z. Mahmoud, R. Jäger, M. Grabherr, R. Michalzik, and K.J. Ebeling, “Large-area single-mode VCSELs and the self-aligned surface relief”, *IEEE J. Select. Topics Quantum Electron.*, vol. 7, no. 2, pp. 386–392, 2001.
- [12] A. Larsson and J.S. Gustavsson, “Single-Mode VCSELs”, Chap. 4 in *VCSELs — Fundamentals, Technology and Applications of Vertical-Cavity Surface-Emitting Lasers*, R. Michalzik (Ed.), Springer Series in Optical Sciences, vol. 166, 26 pages. Berlin: Springer-Verlag, 2012, in press.
- [13] A. Kroner, F. Rinaldi, J.M. Ostermann, and R. Michalzik, “High-performance single fundamental mode AlGaAs VCSELs with mode-selective mirror reflectivities”, *Optics Commun.*, vol. 270, pp. 332–335, 2007.
- [14] J.M. Ostermann, F. Rinaldi, P. Debernardi, and R. Michalzik, “VCSELs with enhanced single-mode power and stabilized polarization”, *IEEE Photon. Technol. Lett.*, vol. 17, no. 11, pp. 2256–2258, 2005.
- [15] M. Peeters, K. Panajotov, G. Verschaffelt, B. Nagler, J. Albert, H. Thienpont, I. Veretennicoff, and J. Danckaert, “Polarisation behavior of vertical-cavity surface-emitting lasers under the influence of in-plane anisotropic strain”, in *Vertical-Cavity Surface-Emitting Lasers VI*, Proc. SPIE 4649, pp. 281–291, 2002.